RESONANT FREQUENCIES OF HIGHER ORDER MODES IN CYLINDRICAL ANISOTROPIC DIELECTRIC RESONATORS

Michael E. Tobar and Anthony G. Mann

Department of Physics, University of Western Australia, Nedlands 6009, Australia.

Abstract: An improved method is developed which allows the determination of mode frequencies to high accuracy in cylindrical anisotropic dielectric resonators. This is an extension of Garault and Guillon's method from isotropic to anisotropic dielectrics, applied to four different classes of field patterns. Application to high Q sapphire crystal resonators is discussed.

INTRODUCTION

A method which calculates the frequency of the lowest order mode in an cylindrical isotropic dielectric (1) has been extended to higher order modes in an anisotropic crystal. Previous equations are shown only to be valid for quasi TE modes with even mode number in the axial direction. Four different axial match equations are derived depending whether they are quasi TE or quasi TM, and have an odd or even axial mode number. A general radial match equation is derived. Combining it with the relevant axial equation forms a set of two coupled transcendental equations which can be be solved numerically. To the authors' knowledge this is the first general treatment of higher order modes in an anisotropic medium, although previously a whispering gallery mode approximation for anisotopic crystals has been used successfully (2).

Theory is applied to two sapphire crystals of different aspect ratios. Very good agreement is found even though the permittivity is only about ten. The anisotropy forces the TM mode families to be lower in frequency than the TE, which explains the discrepancy between theory and experiment of previous work (3).

At cryogenic temperatures sapphire resonators can exhibit extremely high Q's ($>10^7$) and can be used to construct ultra-stable low noise microwave oscillators (3) (4) (5) (6). The theory presented successfully predicts frequency shifts from room to liquid helium temperature due to the change in permittivity, and the tuning range of a tunable sapphire resonator due to the effective change in height.

THEORY

Cylindrical anisotropic crystals in free space are analysed relative to the coordinate system defined in figure 1, with the c-axis of the crystal parallel to the z axis. The permittivity parallel and perpendicular to the c-axis is defined as ε_z and ε_r respectively. Thus $\varepsilon_\phi = \varepsilon_r$ and we assume no off diagonal terms in the permittivity tensor.

The problem is solved using Maxwell's equations for anisotropic media. Applying separation of variables on the z component of the electromagnetic field, we can write;

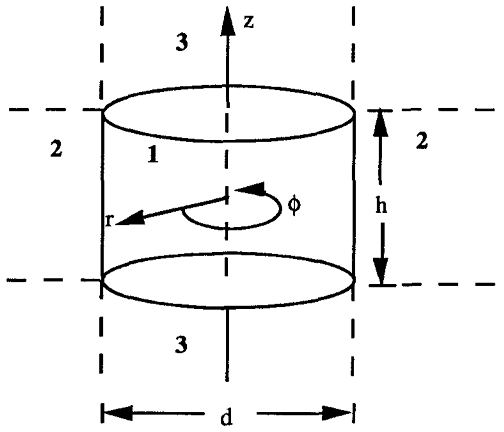

Fig.1 The open dielectric crystal is analysed in cylindrical coordinates {r,ϕ,z}. Resonant frequencies are solved by matching tangential fields between regions 1 and 2, and regions 1 and 3.

$$E_{z1} = A\,J_m(k_E r)\begin{matrix}\mathrm{Cos}(m\phi)\\ \mathrm{Sin}(m\phi)\end{matrix}\left(P_1\exp(-j\beta z) + P_2\exp(+j\beta z)\right) \quad 1a$$

$$E_{z2} = C\,K_m(k_{out} r)\begin{matrix}\mathrm{Cos}(m\phi)\\ \mathrm{Sin}(m\phi)\end{matrix}\left(P_1\exp(-j\beta z) + P_2\exp(+j\beta z)\right) \quad 1b$$

$$E_{z3} = E\,J_m(k_E r)\begin{matrix}\mathrm{Cos}(m\phi)\\ \mathrm{Sin}(m\phi)\end{matrix}\exp(-\alpha z) \quad 1c$$

$$H_{z1} = B\,J_m(k_H r)\begin{matrix}\mathrm{Sin}(m\phi)\\ \mathrm{Cos}(m\phi)\end{matrix}\left(P_1\exp(-j\beta z) + P_2\exp(+j\beta z)\right) \quad 1d$$

$$H_{z2} = D\,K_m(k_{out} r)\begin{matrix}\mathrm{Sin}(m\phi)\\ \mathrm{Cos}(m\phi)\end{matrix}\left(P_1\exp(-j\beta z) + P_2\exp(+j\beta z)\right) \quad 1e$$

$$H_{z3} = F\,J_m(k_H r)\begin{matrix}\mathrm{Sin}(m\phi)\\ \mathrm{Cos}(m\phi)\end{matrix}\exp(-\alpha z) \quad 1f$$

where $k_E^2 = \varepsilon_z k_0^2 - \beta^2$, $k_H^2 = \varepsilon_r k_0^2 - \beta^2$ and $k_{out}^2 = \beta^2 - k_0^2$. Here m is the azimuthal mode number, β the longitudinal dielectric propagation constant, k_0 the free space wave number, k_{out} the radial propagation constant outside the dielectric, and k_E and k_H the radial dielectric propagation constants parallel and perpendicular to the c-axis respectively. From the z component, Maxwell's equations can then be used to obtain all other electromagnetic field components (7).

CH2870-4/91/0000-0143$01.00 © 1991 IEEE

Radial Match

By matching tangential components of the H and E fields between regions 1 and 2, the following transcendental equation is obtained;

$$\left(\frac{\varepsilon_r J'_m(x_E)\, x_E}{x_H^2 J_m(x_E)} + \frac{K'_m(y)}{y\, K_m(y)}\right)\left(\frac{J'_m(x_H)}{x_H J_m(x_H)} + \frac{K'_m(y)}{y\, K_m(y)}\right)$$

$$= m^2 \frac{\left(x_H^2+\varepsilon_r y^2\right)\left(x_H^2+y^2\right)}{x_H^4\, y^4} \qquad 2$$

where $x_E = k_E\, d/2$, $x_H = k_H\, d/2$ and $y = k_{out}\, d/2$. For a fixed diameter this equation is a function of two variables, k_0 and β.

In general y becomes imaginary for the lower order whispering gallery mode families. In this case the Evanescent Bessel Function becomes a Hankel Function of the second kind (8). Hence we employ algorithms which allow complex arguments.

Axial Match

Field components E_z and H_z must be orthogonal in space and hence can not co-exist with the same dependance on z. Assuming the same dependance simplifies proceedings by allowing the axial match to be calculated independently of the radial match. To be consistent with the z dependance in eqn. 1a to eqn. 1f, quasi TE modes ($E_z \approx 0$) or quasi TM modes ($H_z \approx 0$) must be assumed. Four different transcendental equations are derived by matching tangential fields between regions 1 and 3. The radial and axial mode numbers are n and p respectively.

$TE_{m\,n\,p+\delta}$ p even; $$k_0^2 = \beta^2\, \frac{1+\mathrm{Tan}^2(\beta\, h/2)}{\varepsilon_r - 1} \qquad 3a$$

p odd; $$k_0^2 = \beta^2\, \frac{1+\mathrm{Cot}^2(\beta\, h/2)}{\varepsilon_r - 1} \qquad 3b$$

$TM_{m\,n\,p+\delta}$ p even; $$k_0^2 = \beta^2\, \frac{1+\left(\mathrm{Tan}(\beta\, h/2)/\varepsilon_r\right)^2}{\varepsilon_z - 1} \qquad 3c$$

p odd; $$k_0^2 = \beta^2\, \frac{1+\left(\mathrm{Cot}(\beta\, h/2)/\varepsilon_r\right)^2}{\varepsilon_z - 1} \qquad 3d$$

Eqn. 3a is the same as derived by Garault and Guillon (1), which was solved with the isotropic version of Eqn. 2.

Solving the coupled equations

Eqn. 2 and 3 are solved using Mathematica (9). Solutions are found graphically on a x_H^2 versus y^2 graph, then more accurately using a Newton Raphson technique. For a given value of m, eqn. 2 gives an infinite set of solutions in $\{x_H^2, y^2\}$ space, which are almost perpendicular to the x_H^2 axis. This distinguishes the value of n, and whether they are TE or TM. Eqn. 3 gives a infinite set of solutions nearly parallel to the x_H^2 axis. Mode frequencies are solved from the intersection of these two solution sets. Care must be taken to avoid spurious solutions due to the restriction of p being either even or odd.

EXPERIMENTAL VERIFICATION

Cylindrical oriented sapphire

Fig. 2 shows how quasi TE and TM modes are distinguished. To excite a TM or TE mode an E_z or H_z field is excited respectively. Analysis of azimuthal and axial mode numbers is done by observing the H_ϕ or E_ϕ field respectively.

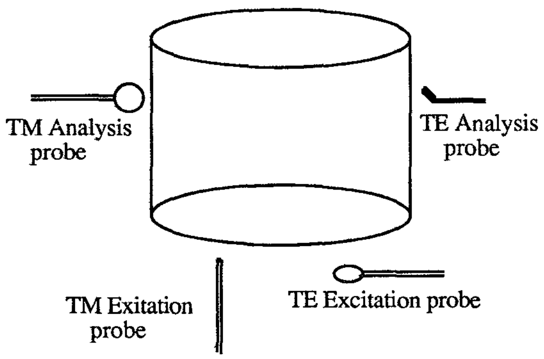

Fig 2. TM modes are excited by creating a E_z field, while TE modes are excited by creating a H_z field.

Analysis of resonant modes is conducted over X-Band for two cylindrical pieces of sapphire with different aspect ratios. Fig. 3 and fig. 4 compare experimental and theoretical mode frequencies, and observed open resonator Q values. There is better agreement for the whispering gallery type families of low axial mode number p, as they are more TM or TE like. In reality all modes are hybrid and experimentally one can excite higher order families with either a TM or TE probe. Percentage difference between calculated and measured frequencies are presented in tables 1 and 2. For modes with p=0 errors are less than .1% which lies within estimated errors due to uncertainties in permittivities and dimensions. Above p=2 errors can be of the order 1% .

The permittivity of sapphire above and below X-band has been measured previously with slightly conflicting results (10) (11). To be consistent with both reports we can be confident that ε_z is 11.6245±.0355 and 11.355±.015 at 300 K and 4 K respectively, and ε_r is 9.407±.012 and 9.2895±.0255 at 300 K and 4 K respectively.

For each mode family, the power radiated from an open dielectric resonator decreases as the azimuthal mode number increases. Hence the observed open resonator Q increases monotonically to the room temperature limit of about $2 \cdot 10^5$, due to intrinsic crystal losses. Some modes don't follow this pattern as a nearby mode maybe reactively coupled. This will cause the Q of the lower Q mode to increase at the expense of the other degrading (12). For the 50 mm diameter sapphire the density of modes in the 11 GHz region is large and interacting modes are common. In this region the mode Q curves may decrease in Q for an increase in azimuthal mode number.

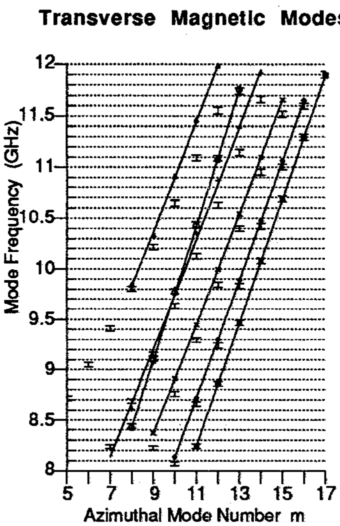

fig. 3a

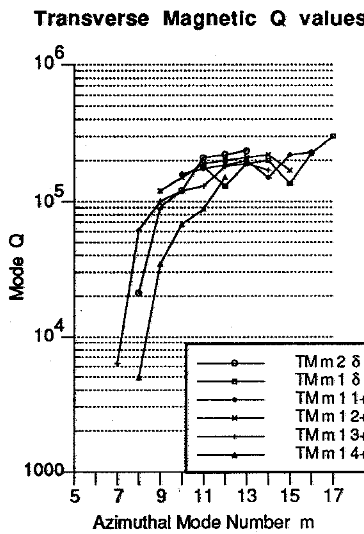

fig. 3b

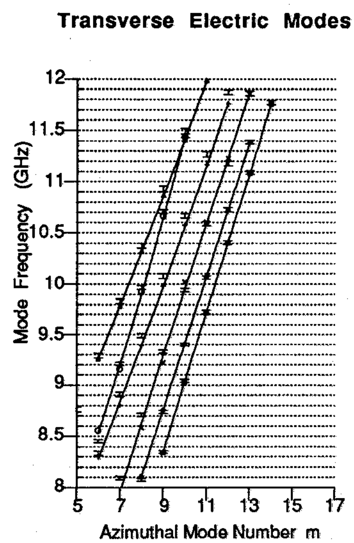

fig. 3c

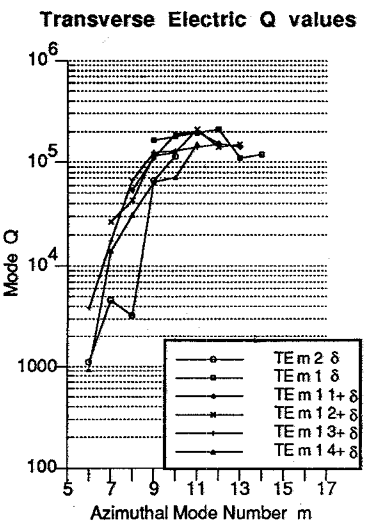

fig. 3d

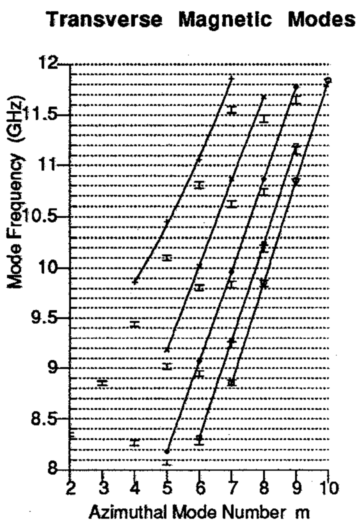

fig. 4a

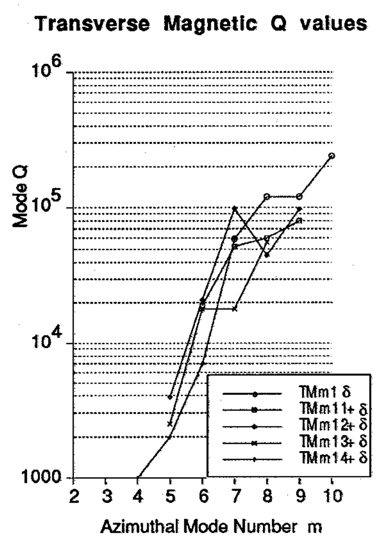

fig. 4b

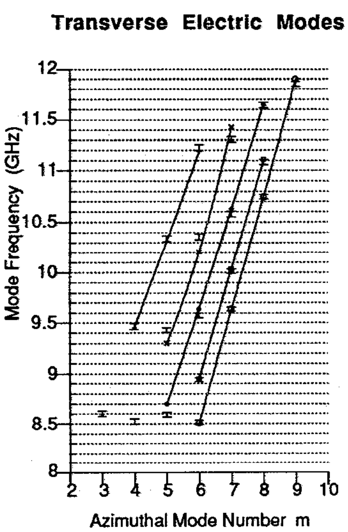

fig. 4c

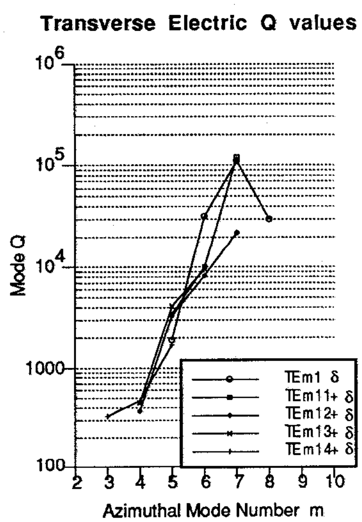

fig. 4d

Fig. 3 and 4 show Transverse Magnetic and Electric mode frequencies and Q values as a function of azimuthal mode number. Theoretical points are plotted as error bars due to uncertainties in dimensions and permittivities, while experimental points are joined by lines. Fig. 3 is for a d = 50.0 mm and h = 30.0 mm sapphire crystal. Fig. 4 is for a d = 31.8 mm and h = 30.2 mm sapphire crystal.

m	n=2 p=0	n=1 p=0	p=1	p=2	p=3	p=4
7					-0.219	
8	-0.209				-0.910	0.415
9	-0.135			1.73	-0.962	1.15
10	-0.123		0.800	1.70	1.78	2.46
11	-0.0786	-0.0239	0.710	1.61	2.19	3.27
12	-0.115	0.000678	0.656	1.50	2.24	3.67
13	0.130	-0.00306	0.601	1.40	2.18	
14		-0.000994	0.547	1.30	2.12	
15		-0.0627	0.505	1.20		
16		0.0319	0.454			
17		-0.0555				

Table 1. Percentage difference between theoretical and experimental TM mode frequencies for the 50.0 mm diameter sapphire.

m	n=2 p=0	n=1 p=0	p=1	p=2	p=3	p=4
6	1.19				-0.411	-0.352
7	-0.600			-1.33	-1.21	-0.495
8	-0.416		0.429	-1.46	-1.06	-0.535
9	-0.430	-0.0920	0.152	-1.20	-0.976	-0.558
10	-0.0926	-0.0820	0.0657	0.802	-0.905	-0.694
11		-0.0718	0.0308	0.144	-0.884	-0.607
12		-0.0557	0.00746	0.428	-0.938	
13		-0.0550	-0.000871	-0.0632		
14		-0.0689				

Table 2. Percentage difference between theoretical and experimental TE mode frequencies for the 50.0 mm diameter sapphire.

Applications to Sapphire Loaded Superconducting Cavities (SLOSC)

Details of a high stability 9.73 GHz SLOSC oscillator have been presented previously (4) (5). The operational sapphire resonance can now be identified as $TE_{6\,1\,\delta}$. Theory predicts a 66 MHz shift in frequency when cooled due to the change in dielectric constant, exactly what is measured.

Details of a tunable SLOSC have been presented previously (12) (13). It consists of a 3 cm diameter cylindrical sapphire crystal, and an axially driven tuning disc .3 cm thick. Tuning ranges can be predicted with presented theory. Modes with higher tuning ranges have larger axial mode numbers. Modes analysed previously (12) at 4 K are now identified as $TE_{6\,1\,\delta+1}$ at 10.221 GHz and $TM_{8\,1\,\delta+1}$ at 10.44 GHz. Tuning ranges of these modes are predicted to be 72 and 99 MHz respectively, which agrees favorably with experiment.

CONCLUSION

Improved theory for multimode analysis of anisotropic dielectric resonators was presented. This has lead us to a very good understanding of electromagnetic resonances in sapphire crystals, with potential application to design.

ACKNOWLEDGMENTS

The authors would like to thank Dr. Steve Jones whose ideas initiated this research. This research was supported by the Australian Research Council.

REFERENCES

(1) Y. Garault and P. Guillon, "Higher accuracy for the resonance frequencies of dielectric resonators," Electron. Lett., Vol. 12, No. 18, pp. 475-476, Sept. 1976

(2) S.N. Bun'kov et al, "Cooled dielectric resonators for frequency stabilization," Radiotekhnika i elektronika, No. 5, pp. 1071-1080, 1987.

(3) G.J. Dick and J. Saunders, "Measurement and analysis of a microwave oscillator stabilized by a sapphire dielectric ring resonator for ultra low noise" IEEE Trans. Ultrason. Ferroelec. Freq. Contr., Vol. 37, No.5, pp. 339-346, Sept. 1990.

(4) A.J. Giles, S.K. Jones, D.G. Blair and M.J. Buckingham, "A high stability microwave oscillator based on a sapphire loaded superconducting cavity," in Proc. 43rd Annu. Symp. Freq. Contr., 1989. pp. 89-93.

(5) A.J. Giles, A.G. Mann, S.K. Jones, D.G. Blair and M.J. Buckingham, "A very high stability sapphire loaded superconducting cavity oscillator," Physica B, 165, pp. 145-146, 1990.

(6) M.E. Tobar and D.G. Blair, "Analysis of an ultra low phase noise tunable oscillator based on a tunable sapphire loaded superconducting cavity resonator," to be published in Proc. 45th Annu. Symp. Freq. Contr., 1991.

(7) H. Auda and D. Kajfez, "Dielectric rod waveguides," in *Dielectric Resonators,* D. Kajfez and P. Guillon, Ed., Artech House, Inc., 1986 pp. 65-111.

(8) J.R. Wait, "Electromagnetic whispering gallery modes in a dielectric rod," Radio Science, Vol. 2, No. 9, pp. 1005-1017, Sept. 1967.

(9) S. Wolfram, *Mathematica a system for doing mathematics by computer.* Addison-Wesley, 1988.

(10) E. Loewenstein, D. Smith and R. Morgan, "Optical constants of far infrared materials," Appl. Opt. 12, 398, 1973.

(11) R. Shelby and J. Fontanella, "The low temperature electrical properties of some anisotropic crystals," J. Phys. Chem. Solids, Vol. 41, pp. 69-74, 1980.

(12) M. Tobar and D. Blair, "A generalized equivalent circuit applied to a tunable superconducting resonator," Submitted to IEEE Trans. Microwave Theory Tech.

(13) D. Blair and A. Sanson, "High Q tunable sapphire loaded cavity resonator for cryogenic operation," Cryogenics, Vol. 29, Nov. 1989. pp. 1045-1049.